NANO LETTERS

2006
Vol. 6, No. 4
839−842

Near-Field Electrospinning

Daoheng Sun,[†,‡] Chieh Chang,[†] Sha Li,[†] and Liwei Lin*[,†]

Department of Mechanical Engineering and Berkeley Sensor and Actuator Center, University of California, Berkeley, California 94720, and Department of Mechanical and Electrical Engineering, Xiamen University, China

Received February 6, 2006; Revised Manuscript Received March 9, 2006

Downloaded via UNIV OF ALABAMA BIRMINGHAM on November 24, 2018 at 08:45:41 (UTC).
See https://pubs.acs.org/sharingguidelines for options on how to legitimately share published articles.

ABSTRACT

A near-field electrospinning (NFES) process has been developed to deposit solid nanofibers in a direct, continuous, and controllable manner. A tungsten electrode with tip diameter of 25 μm is used to construct nanofibers of 50–500 nm line width on silicon-based collectors while the liquid polymer solution is supplied in a manner analogous to that of a dip pen. The minimum applied bias voltage is 600 V, and minimum electrode-to-collector distance is 500 μm to achieve position controllable deposition. Charged nanofibers can be orderly collected, making NFES a potential tool in direct write nanofabrication for a variety of materials.

Electrically driven liquid jets and the stability of electrically charged droplets have been studied for hundreds of years,[1,2] while the practical apparatus of electrospinning, in which a charged jet of polymer solution is deposited onto a collector under the influence of an electrical field, dated back in 1934.[3] The feasibility to construct long and continuous polymeric,[4−6] ceramic,[7] and composite[8] nanofibers as well as nanotubes[9] with diameters less than 100 nm has been demonstrated using electrospinning. Typical applications include bioscaffolding,[10] wound dressing,[11] and filtrations[12] to name a few. Researchers have further explored the possibilities of using electrospun nanofibers in fabricating micro- and nanodevices such as field effect transistors,[13] gas[14] and optical sensors,[15] and deposition of DNA on functional chips.[16] In these and other applications, the controllability of the electrospinning process is critical. Unfortunately, current setup of electrospinning is unstable in nature as it relies on the chaotic whipping of liquid jets to generate nanofibers. Limited works toward the control of electrospinning have emerged, including aligning nanofibers by electrical field[17] and using rotational mechanical mandrels.[18,19] Furthermore, numerous investigations by means of analytical and experimental methodologies have been conducted to study the fundamental physics and chemistry of electrospinning for further improvement and control, such as the effects of polymer solution concentration, applied voltage, and electrode-to-collector distance.[4,20−22] Here we report experiments of controllable electrospinning based on a new type of "near-field" electrospinning (NFES). Figure 1A illustrates the schematic setup of NFES that merges several disparate concepts. First, the electrode-to-collector distance, h, is in the range of 500 μm to 3 mm to utilize the stable liquid jets region for controllable deposition. Second, a solid tungsten spinneret of 25 μm tip diameter as illustrated in Figure 1B is used in NFES to achieve nanofibers with sub-100-nm resolution. Third, the applied electrostatic voltage is reduced due to the short electrode-to-collector distance while the electrical field in the tip region maintains the strength in the range of 10^7 V/m as those used in conventional electrospinning to activate the process. Fourth, discrete droplets of polymer solution are supplied in a manner analogous to that of a dip pen by immersing and pulling the tungsten electrode in to and out of the polymer solution. Figure 1C shows that a droplet of 50 μm in diameter is extracted from the polymer solution under an optical microscope for NFES. A Taylor cone is observed under an optical microscope during the process of NFES as shown in Figure 1D. As the process proceeds, the polymer solution on the tungsten tip is consumed and its diameter shrinks, leading to a smaller Taylor cone and thinner nanofibers as observed in Figure 1E.

NFES is not the only direct-write, "serial" material deposition method for nanofabrication. For example, DPN[23] which uses an atomic force microscope tip to deliver collections of molecules to a solid substrate via capillary transport can deposit materials of better than 30 nm line width with fine position control. This is an advantage over conventional electrospinning, unless one is trying to make large area, continuous, and fast deposition. Inkjet printing,[24] on the other hand, can make large area and fast deposition with discrete droplets of size in the micrometer range. The controllability of deposition location is again an advantage over conventional electrospinning unless one is trying to have continuous and submicrometer line-width resolution. In these regards, NFES complements DPN, inkjet, and conventional electrospinning by providing the feasibility of controllable electrospinning for sub-100-nm nanofabrication.

* Corresponding author. E-mail: lwlin@me.berkeley.edu.
[†] University of California.
[‡] Xiamen University.

10.1021/nl0602701 CCC: $33.50 © 2006 American Chemical Society
Published on Web 03/22/2006

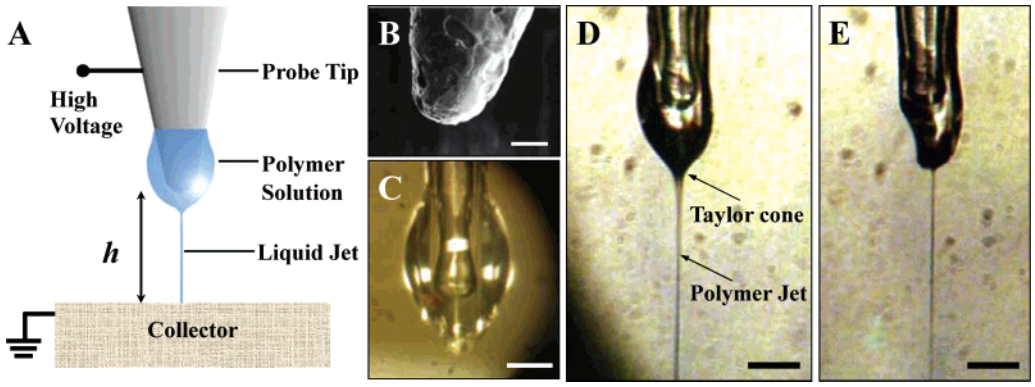

Figure 1. (A) Schematic representation of NFES. The polymer solution is attached to the tip of the tungsten electrode in a manner analogous to that of a dip pen. (B) SEM photomicrograph showing the tip region of the tungsten electrode used in the experiment with a tip diameter of 25 μm. Scale bar, 10 μm. (C) An optical photo showing a 50 μm diameter polymer solution droplet attached on the tip of the tungsten electrode. Scale bar, 20 μm. (D) A polymer jet is ejected from the apex of a Taylor cone under applied electrical field and observed under an optical microscope. Scale bar, 25 μm. (E) The size of the polymer droplet decreases as the polymer jet continues to electrospin. Scale bar, 25 μm.

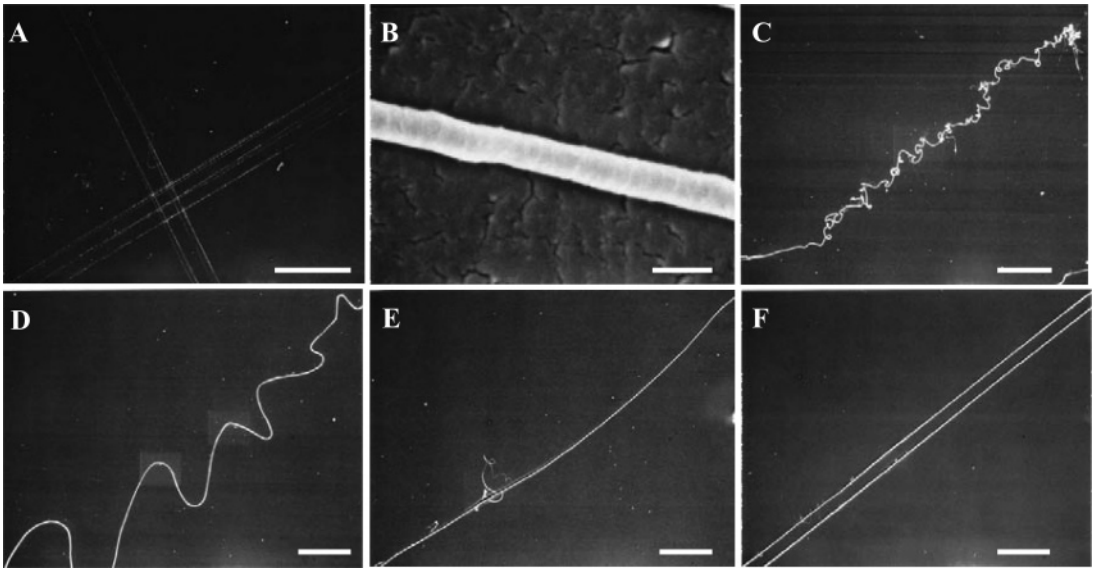

Figure 2. (A) Two groups of parallel lines constructed perpendicular to each other by NFES. Scale bar, 1 mm. (B) Enlarged SEM photomicrograph showing a nanofiber with diameter of 300 nm. Scale bar, 500 nm. (C) NFES result when the collector has a moving speed of 5 cm/s showing "local spiraling". Scale bar, 100 μm. (D) Collector moving speed at 10 cm/s. Scale bar, 100 μm. (E) Collector moving speed at 15 cm/s. Scale bar, 100 μm. (F) Collector moving speed is 20 cm/s, and straight lines can be constructed. The two nanofibers are separated 25 μm away from each other under the control of the $x-y$ stage. Scale bar, 100 μm.

Although there are various choices of nanofiber material and collector systems, we focus on the deposition of poly(ethylene oxide) (PEO, $M_v = 300\,000$), a polymer that has been studied extensively in electrospinning onto silicon-based collectors for possible system integration with MEMS (microelectromechanical systems) and microelectronics. All experiments are conducted under room temperature and 1 atm pressure. During electrospinning, adequate electro-to-collector distance is required to allow solvent to evaporate and nanofibers to become thinner via the whipping and splitting processes.[25] NFES takes the advantage of a stable liquid jet region immediately outside the spinneret for position controllable deposition by shortening the electrode-to-collector distance. At the same time, an electrode with a fine tip is introduced to generate (1) intensified electrical field to activate electrospinning, and (2) small-diameter liquid jets in the stable region. In a typical NFES process of 5 s, a single nanofiber with a length of several centimeters can be constructed. The droplet size, polymer solution concentration, applied voltage, and the electrode-to-collector distance collectively affect the morphology of the electrospun nanofibers. Overall, the near field electrospun solid nanofibers have similar morphology as the conventional electrospinning process while further studies are necessary to characterize these various factors. The controllability of nanofibers is demonstrated by moving the collector along a straight line to generate line-shape nanofibers. Figure 2A shows an example where parallel lines perpendicular to each other are constructed using an $x-y$ stage (Nano Workcell, Adept Japan Inc.) to control the collector movement. In this experiment, the electrode-to-collector distance is 1 mm, applied voltage is 1000 V, and PEO solution is 5 wt %. The close view scanning electron microscopy (SEM) photomicrograph in Figure 2B shows that the typical diameter of the nanofiber

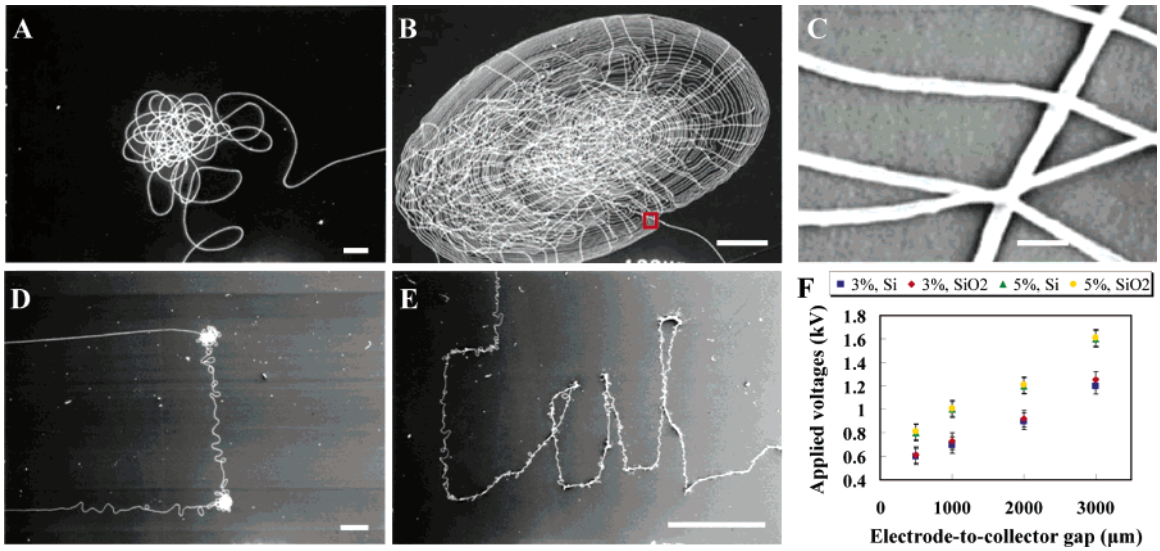

Figure 3. (A) When the collector is stationary for 0.5 s while making a 90° turn, the local spiraling effect is observed as the result of self-expelling as nanofibers are electrically charged. The spread is in the range of 50 μm in diameter. Scale bar, 10 μm. (B) When the substrate is covered with an electrical isolation layer of silicon dioxide, the local spiraling is enhanced as the concentric/elliptical rings are formed in an area of about 300 μm in diameter. Scale bar, 100 μm. (C) Close view of (B) showing the distance between the adjacent nanofibers is about 1.5 μm. Scale bar, 1 μm. (D) A "U"-shaped symbol is plotted manually by NFES. Excessive nanofiber depositions are observed at the two corners when the collector stopped shortly for the adjustment of the moving direction. Scale bar, 100 μm. (E) The three-character "Cal" is manually drawn in a period of 3 s. Scale bar, 1 mm. (F) Experimental results on the minimum required voltages vs electrode-to-collector distance to activate the NFES process under various polymer concentrations on either silicon or silicon oxide collectors.

by NFES is 300 nm. More controllability is illustrated in parts C, D, and E of Figure 3 when the collector is moving along a straight line with speeds of 5, 10, and 15 cm/s, respectively. In these cases, the nanofiber electrospinning speed is faster than the collector moving speed. The result is that "local spiraling" occurs as in Figure 3C and gradually diminishes as the collector is moving faster in parts D and E of Figure 3. When the collector speed reaches 20 cm/s as shown in Figure 3F, straight-line-shape nanofibers can be constructed. In this case, we control the $x-y$ stage to deposit two straight nanofibers 25 μm away from each other.

The location of the nanofiber formation under NFES is investigagted by keeping the spinnert and collector stationary. It is observed that in a period of less than 1 s without moving the collector, the NFES deposition is concentrated within a short radial distance of 50 μm as seen in Figure 3A. The local spiraling is the result of the self-expelling of nanofibers as they are electrically charged. This demonstrates the feaibility of locational control of NFES on a conductive collector while conventional electrospinning will result in widespread and random deposition. Figure 3B shows a 2-s NFES deposition result on a stationary, 2 μm thick insulating oxide-coated silicon substrate collector. Although the collector does not move, concentric and elliptical patterns of nanofibers are constructed as shown and cover an area with base length of more than 300 μm. The close view SEM photomicrograph in Figure 3C shows that the typical distance between adjacent nanofibers is about 1.5 μm and is somehow relatively uniform over the whole pattern with no external control. Parts D and E of Figure 3 further illustrate the controllability of NEFS under manual operations. Figure 3D shows that a "U"-shaped nanofiber is generated under one single NFES process. A straight line is plotted to construct the top line of the "U"-shaped structure. Afterward, the collector stops to change to the downward direction and stops again before moving leftward. It is shown that during each stop of less than 0.5 s the continuous deposition of nanofibers causes accumulation at the corners. We purposely slow the collector moving speed to draw the middle and bottom portion of the "U"-shaped symbol, and the "local spiraling" occurs as charged nanofiber expel each other when excessive nanofibers are to be deposited on the same location. Figure 3E shows an attempt to manually draw more complicated characters such as "Cal" in one single NFES process. Each character is about 1×2 mm^2 in size and it takes about 1 s to manually write one character. The writing speed is not fast enough to have clean shape under the manual control. We conclude that location and pattern control of NFES are achievable to deposit nanofibers without spiraling effects when the relative moving speed between the spinneret and collector is comparable to the electrospinning speed that is determined by various factors, including the viscosity, conductivity and surface tension of the polymer solution, applied electrical field, tip diameter of the spinneret, the size of the droplet, and ambient parameters including temperature, humidity, and air velocity. Further investigations are required to characterize these effects quantitatively.

Figure 3F shows experiments on the minimum required voltages versus electrode-to-collector distances to activate NFES under various polymer concentrations and types of collectors when the polymer droplets have a nominal size of 50 μm in diameter. The minimum applied voltage increases when either the electrode-to-collector distance or the polymer solution concentration increases. We have

performed an electrostatic field simulation using FEMLab with either a 500 μm thick silicon wafer or a 500 μm thick silicon wafer coated with a 2 μm thick silicon dioxide. Simulation results indicate that the electrical field around the tungsten tip is around 5×10^7 and 7×10^7 V/m for the 3 and 5 wt % PEO concentration experiments, respectively, independent of the electrode-to-collector distance. The magnitudes of the electrical field for the collectors with and without the oxide insulating layer are similar under the same applied bias as the thin oxide layer does not affect the electrical field strength significantly. Furthermore, it is observed that nanofibers collected on silicon collector are nominally bigger than those on the oxide-coated collector under the same deposition condition since nanofibers travel a longer distance on average (Figure 3B) and have more time for the solvent to evaporate. Statistical results show that when the electrode-to-collector distance is 500 μm with 3 wt % PEO, the diameters of nanofiber on the silicon and oxide-coated silicon collector are in the range of 150−300 nm and 50−200 nm, respectively.

NFES is a simple yet powerful method for direct-write deposition of nanofibers with unprecedented controllability at resolutions comparable to those achieved with much more expensive and sophisticated lithography tools. It should be especially useful for the heterogeneous integration of nanoscale materials to devices prepared by conventional lithographic and manufacturing methods, such as microelectronics and MEMS structures. Furthermore, NFES could play a key role in building up larger-area, ordered nonwoven nanofibers for various applications.

Acknowledgment. The authors thank Mr. Ron Wilson for assistance with the SEM work. D.S. was supported by the Berkeley China Scholarship Program and C.C. is supported in part from NSF Grant EEC-0425914.

References

(1) Rayleigh, L. *London, Edinburgh, Dublin Philos. Mag. J.* **1882**, *44*, 184.
(2) Zeleny, J. *Phys. Rev.* **1917**, *10*, 1
(3) Formhals, A. US Patent 1,975,504, 1934.
(4) Reneker, D. H.; Chun, I. *Nanotechnology* **1996**, *7*, 216.
(5) Li, D.; Xia, Y. *Adv. Mater.* **2004**, *16*, 1151.
(6) Zhou, Y.; Freitag, M.; Hone, J.; Staii, C.; Johnson, A. T., Jr.; Pintod, N. J.; MacDiarmide, A. G. *Appl. Phys. Lett.* **2003**, *83*, 3800.
(7) Dai, H.; Gong, J.; Kim, H.; Lee, D. *Nanotechnology* **2002**, *13*, 674.
(8) Bergshoef, M. M.; Vancso, G. J. *Adv. Mater.* **1999**, *11*, 1362.
(9) Ko, F.; Gogotsi, Y.; Ali, A.; Naguib, N.; Ye, H.; Yang, G. L.; Li, C.; Willis, P. *Adv. Mater.* **2003**, *15*, 1161.
(10) Li, W.-J.; Laurencin, C. T.; Caterson, E. J.; Tuan, R. S.; Ko, F. K. *J. Biomed. Mater. Res.* **2002**, *60*, 613.
(11) Min, B.-M.; Lee, G.; Kim, S. H.; Nam, Y. S.; Lee, T. S.; Park, W. H. *Biomaterials* **2004**, *25*, 1289.
(12) Gibson, P.; Schreuder-Gibson, H.; Riven, D. *Colloids Surf., A* **2001**, *187*, 469.
(13) Pinto, N. J.; Johnson, A. T., Jr.; MacDiarmid, A. G.; Mueller, C. H.; Theofylaktos, N.; Robinson, D. C.; Miranda, F. A. *Appl. Phys. Lett.* **2003**, *83*, 4244.
(14) Liu, H.; Kameoka, J.; Czaplewski, D. A.; Craighead, H. G. *Nano Lett.* **2004**, *4*, 671
(15) Wang, X.; Drew, C.; Lee, S.-H.; Senecal, K. J.; Kumar, J.; Samuelson, L. A. *Nano Lett.* **2002**, *2*, 1273.
(16) Takahashi, T.; Taniguchi, M.; Kawai, T. *Jpn. J. Appl. Phys.* **2005**, *44*, L860
(17) Li, D.; Ouyang, G.; McCann, J. T.; Xia, Y. *Nano Lett.* **2005**, *5*, 913.
(18) Theron, A.; Zussman1, E.; Yarin, A. L. *Nanotechnology* **2001**, *12*, 384.
(19) Kameoka, J.; Orth, R.; Yang, Y.; Czaplewski, D.; Mathers, R.; Coates, G. W.; Craighead, H. G. *Nanotechnology* **2003**, *14*, 1124.
(20) Frenot, A.; Chronakis, I. S. *Curr. Opin. Colloid Interface Sci.* **2003**, *8*, 64.
(21) Huang, Z.-M.; Zhang, Y.-Z.; Kotaki, M.; Ramakrishna, S. *Compos. Sci. Technol.* **2003**, *63*, 2223.
(22) Son, W. K.; Youk, J. H.; Lee, T. S.; Park, W. H. *Polymer* **2004**, *45*, 2959.
(23) Piner, R. D.; Zhu, J.; Xu, F.; Hong, S.; Mirkin, C. A. *Science* **1999**, *283*, 661.
(24) Sirringhaus, H.; Kawase, T.; Friend, R. H.; Shimoda, T.; Inbasekaran, M.; Wu, W.; Woo, E. P. *Science* **2000**, *290*, 2123.
(25) Reneker, D. H.; Yarin, A.; Fong, H.; Koombhongse, S. *J. Appl. Phys.* **2000**, *87*, 4531.

NL0602701